Density functional study on the mechanism of the Simmons–Smith reaction

Thomas K. Dargel and Wolfram Koch*

Institut für Organische Chemie, Technische Universität Berlin, Straße des 17. Juni 135, D-10623 Berlin, Germany

Quantum chemical calculations based on density functional theory (DFT) including relativistic effects either through relativistic core potentials or an explicit, quasi-relativistic approach were used to study the mechanism of the Simmons–Smith cyclopropanation reaction. Under the assumption that the reactive organo-zinc–iodine species is monomeric, and neglecting solvent effects, a concerted one-step mechanistic scenario, postulated to be the most likely mechanism in the literature previously, has indeed been identified as the energetically most favourable pathway for the parent reaction of ethene with ICH_2ZnI to give cyclopropane and ZnI_2. The attack of the cyclopropanating agent is electrophilic in character. Depending on the computational model applied, activation energies with respect to the educts are between 48 and 61 kJ mol^{-1}, while the overall reaction is predicted to be exothermic by 140–158 kJ mol^{-1}.

Introduction

The Simmons–Smith[1] reaction is an important, well known synthetic pathway for the preparation of cyclopropanes through the addition of a carbenoid to a carbon–carbon double bond. The use of a carbenoid instead of a free carbene leads to a decreased reactivity of the reagent and thus suppresses the occurrence of unwanted side products. In the Simmons–Smith reaction the carbenoid is usually generated from CH_2I_2 and a Zn–Cu couple. The only role of the copper has been shown to activate the zinc and its presence is not mandatory for this reaction.[1c] Thus, in the simplest case, the addition of CH_2 to ethene yielding cyclopropane, the Simmons–Smith reaction can formally be summarized as shown in reaction (1). The actual

$$Zn(Cu) + CH_2I_2 + C_2H_4 \longrightarrow C_3H_6 + ZnI_2 \quad (1)$$

attacking species is an organozinc intermediate, however, neither its structure nor whether it is present as a monomer, dimer or oligomer is unambiguously known. As early as 1929 a structure corresponding to 'ICH_2ZnI' was suggested by Emschwiller[2] as being the product of the reaction between activated zinc and CH_2I_2. Other pathways to generate the Simmons–Smith reagents include the reaction of ZnI_2 with CH_2N_2 as suggested originally by Wittig and co-workers[3] and the procedure due to Furukawa and co-workers[4] in which diethylzinc is treated with CH_2I_2. While it is not clear that the reagents formed by each of these methods are identical, their comparable reactivity points to at least closely related methylene transfer reagent structures. However, all attempts to isolate and structurally identify this product failed due to the presence of ZnI_2 and other impurities[1c] and complications due to the presence of Schlenck-type equilibria[1c,d] such as shown in reaction (2).

$$2\ 'ICH_2ZnI' \rightleftharpoons '(ICH_2)_2Zn{-}ZnI_2' \quad (2)$$

In ethereal solution the only structural elements identified were of the form (• • • I–CH_2–Zn–).[1c] Due to the lack of precise knowledge of the structure of active zinc carbenoid, details of how the Simmons–Smith reaction proceeds mechanistically have obviously only been obtained in an indirect fashion.[5] From the fact that the reaction occurs only at the double bond and no isomerized side products are usually found, it was concluded that there is no free carbene intermediate. The absence of any carbanionic intermediates was deduced from the reactions of non-1- and -2-ene, which only yielded heptylcyclopropane and 1-hexyl-2-methylcyclopropane, respectively, and no rearranged products. As already mentioned above, the copper does not play any role in the cyclopropanation reaction itself, which was shown by the fact that the cyclopropanation occurs, even after all the copper has been carefully removed after the preparation of the active carbenoid. Further, the addition is stereospecifically *syn* and no rearranged educt olefin can be found in the reaction mixture. Thus, a reversible coordination between the olefin and the carbenoid, which could lead to isomerization, can be excluded. On the basis of these observations, several mechanistic alternatives can be ruled out.[5] (i) The carbenoid does not attack the double bond as a carbanion, which in a subsequent cyclization could give the cyclopropane derivative. (ii) A mechanism involving radicals as intermediates is highly unlikely due to the observed stereospecificity. (iii) Free carbenes or copper modified carbene species (CH_2 ⟶ Cu) should not contribute to the reaction mechanism. On the other hand, a concerted mechanism as shown in Scheme 1 is consistent with all experimental data and is usually presented in text books[6] as the most likely one. Nevertheless, as of yet no direct information on this mechanism exists as clearly stated by Denmark *et al.*[7] 'Despite the synthetic importance of this reaction, detailed mechanistic understanding and structural characterization of the cyclopropanating species are lacking'. In the following, we apply quantum chemical calculations on the parent Simmons–Smith reaction, *i.e.* the transformation of ethene into cyclopropane by 'ICH_2ZnI', in order to gain a direct insight into the individual steps and to characterize the structure of the active organozinc reagent and the possible saddle points along the reaction coordinate. In order to facilitate our calculations, we have to apply two important simplifications. First, we restricted ourselves to a monomeric species as the active cyclopropanating species and secondly, our calculations apply strictly only to the gas phase, since the influence of a solvent had to be neglected. Obviously,

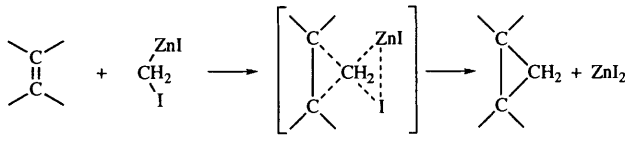

Scheme 1 'Textbook mechanism' of the Simmons–Smith reaction

the degree of dimerization or oligomerization depends on the solvent and the actual reaction conditions. Notwithstanding these two limitations, we believe that our computational study provides for the first time a consistent description of the Simmons–Smith reaction, which not only unravels the details of the gas phase mechanism of the reaction between ethene and ICH_2ZnI but could also serve as a starting point for future investigations.

Methodology

All density functional theory [8] based calculations employed the local density approximation with the local exchange term of Slater [9] and the parametrization of Vosko *et al.* [10] for the correlation contribution of the homogeneous electron gas. This functional was combined with non-local gradient corrections to the exchange functional following Becke [11] and to the correlation part due to Perdew [12] or due to Lee, Yang and Parr. [13] These two functionals will be denoted as BP and BLYP, respectively. All structures have been optimized employing analytical gradients. The force constant matrix and the corresponding harmonic frequencies were computed by numerical differentiation of the analytically determined gradients and used to characterize each stationary point as minima (positive definite force constant matrix) or saddle points (one negative eigenvalue in the force constant matrix). Since the Simmons–Smith reaction involves the very heavy element iodine, relativistic effects have to be accounted for in the calculations. To this end, a relativistic effective core potential (RECP) was utilized for iodine. Zinc was described by a non-relativistic ECP. The (R)ECPs due to Hay and Wadt [14] in the slightly modified form as recommended by Frenking and co-workers [15] have been used. For Zn and I, the innermost 18 and 46 electrons are covered by the (R)ECP, respectively. The remaining valence electrons were described by basis sets of essentially double-zeta quality {Zn: (3s2p5d) ⟶ [2/1,1/1,4/1], I: (3s3p1d) ⟶ [2/1,2/1,1]}. The standard 6-31G* basis set [16] was used for carbon and hydrogen. This (R)ECP–basis set combination has been successfully applied in recent years to a large variety of transition metal chemistry. [17] All these calculations have been performed employing Gaussian 92/DFT. [18] In order to cross check the reliability of the RECP approach to include relativistic effects, we also computed the energies of the stationary points using a quasi-relativistic scheme, as introduced by Ziegler *et al.* [19] and implemented in the ADF program package. [20] While the RECP includes relativistic effects only *en gros* through the parametrization of the core electrons for iodine, the quasi-relativistic approach additionally explicitly accounts for the scalar relativistic effects (mass velocity and Darwin terms) on the valence electrons of all atoms. [19] The ADF calculations also employed the BP functional [11,12] combined with large triple-zeta basis sets, expanded in Slater-type orbitals. The carbon 1s, zinc 1s–2p and iodine 1s–4p electrons were treated in the frozen core approximation. Since the current version (1.1.3) of ADF does not provide analytical gradients in the quasi-relativistic scheme, no geometry optimizations could be performed at this level of theory. Instead, the energies of the optimized structures were computed by employing the BP/RECP method. This level will be denoted as ADF/BP and we expect the so determined energies to be the most reliable ones. Relativistic spin-orbit effects, which are not included in the present treatment, are expected to be of only minor importance, since all species considered are singlet states with closed shells and thus do not exhibit any fine structure splitting or first-order spin-orbit interaction. [21]

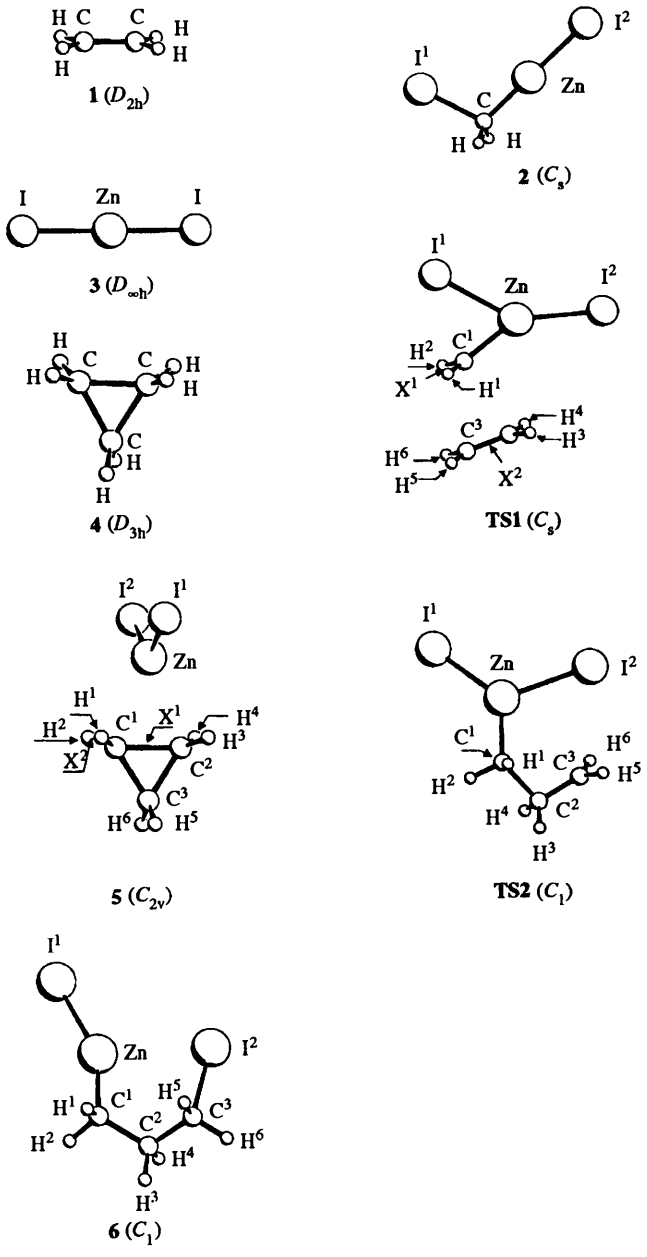

Fig. 1 Species relevant to the Simmons–Smith reaction

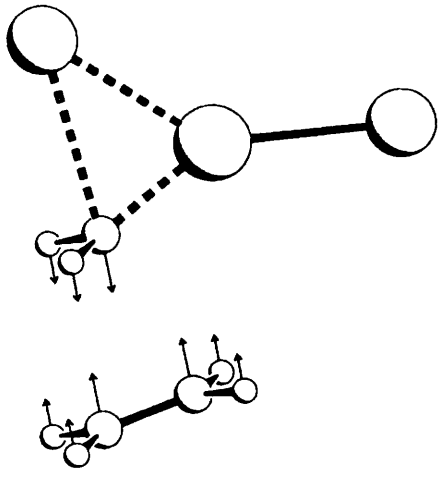

Fig. 2 Transition vector of **TS1**

Results and discussion

Fig. 1 displays the structures and atom numbering of the minima and saddle points localized in our study, while Table 1 summarizes the relevant optimized geometrical parameters together with the corresponding experimental data, where available. The computed total and relative energies are collected in Table 2.

Table 1 Selected calculated and experimental bond distances (r/Å) and bond angles[a] (a/°) of the investigated species

	BP	BLYP	Exp.[a]		BP	BLYP	Exp.[a]
1				**5**			
r[C–C]	1.340	1.341	1.339	r[X^1–Zn]	2.458	2.563	—
r[C–H]	1.097	1.095	1.085	r[C^1–C^2]	1.564	1.566	—
a[H–C–H]	116.3	116.2	117.8	r[C^1–C^3]	1.510	1.516	—
				r[Zn–I^1]	2.549	2.566	—
2				a[C^1–C^3–C^2]	62.4	62.2	—
r[I^1–C]	2.194	2.206	—	a[C^1–C^2–C^3]	58.8	58.9	—
r[C–Zn]	2.013	2.031	—	a[H^1–C^1–H^2]	115.7	115.4	—
r[I^1–Zn]	3.392	3.449	—	a[H^5–C^3–H^6]	115.1	114.9	—
r[Zn–I^2]	2.529	2.549	—	a[I^1–Zn–I^2]	148.6	149.9	—
r[C–H]	1.100	1.097	—				
a[I^1–C–Zn]	107.4	108.9	—	**TS2**			
a[C–Zn–I^2]	180.0	179.4	—	r[I^1–Zn]	2.570	—[b]	—
a[H–C–H]	109.3	109.3	—	r[I^2–Zn]	2.729	—	—
a[H–C–Zn]	114.0	113.3	—	r[C^1–Zn]	2.132	—	—
				r[C^1–C^2]	1.552	—	—
TS1				r[C^2–C^3]	1.468	—	—
r[C^1–Zn]	2.041	2.065	—	a[I^1–Zn–I^2]	126.4	—	—
r[C^1–I^1]	2.680	2.793	—	a[C^1–Zn–I^1]	131.5	—	—
r[C^1–C^2]	2.395	2.383	—	a[C^1–C^2–Zn]	120.1	—	—
r[C^1–X^2]	2.437	2.430	—	a[C^3–C^2–C^1]	99.3	—	—
r[C^1–C^3]	2.658	2.656	—	d[C^1–Zn–I^1–I^2]	−178.1	—	—
r[I^1–Zn]	2.772	2.781	—	d[C^2–C^1–Zn–I^2]	−56.8	—	—
r[I^2–Zn]	2.533	2.556	—	d[C^3–C^2–C^1–Zn]	16.6	—	—
a[C^1–C^2–C^3]	85.5	85.8	—				
a[C^1–C^3–C^2]	63.9	63.5	—	**6**			
a[C^2–C^1–Zn]	95.9	98.7	—	r[I^1–Zn]	2.568	2.588	—
a[I^1–C^1–Zn]	70.4	67.9	—	r[I^2–Zn]	3.052	3.155	—
a[I^1–Zn–I^2]	142.0	141.4	—	r[C^1–Zn]	2.049	2.066	—
a[H^1–C^1–H^2]	112.3	111.7	—	r[C^1–C^2]	1.533	1.539	—
a[X^1–C^1–X^2]	82.3	84.6	—	r[C^2–C^3]	1.525	1.531	—
a[C^1–X^2–C^3]	101.6	102.0	—	a[I^1–Zn–I^2]	111.2	112.4	—
a[H^3–C^2–H^4]	116.2	116.1	—	a[C^1–Zn–I^1]	160.8	161.0	—
Pyram. C_2	8.2	8.6	—	a[C^1–C^2–Zn]	114.2	115.1	—
a[H^5–C^3–H^6]	116.7	116.6	—	a[C^3–C^2–C^1]	116.4	116.8	—
				d[C^1–Zn–I^1–I^2]	172.2	170.0	—
3				d[C^2–C^1–Zn–I^2]	−21.2	−21.9	—
r[Zn–I]	2.502	2.523	—	d[C^3–C^2–C^1–Zn]	57.0	58.3	—
4							
r[C–C]	1.516	1.521	1.510				
r[C–H]	1.095	1.094	1.089				
a[H–C–H]	114.0	113.9	115.1				

[a] Experimental values from: W. J. Hehre, L. Radom, P. v. R. Schleyer and J. A. Pople, *Ab initio Molecular Orbital Theory*, Wiley, New York, 1986. [b] Not computed due to technical problems, see text.

The reaction commences with the interaction of ethene (**1**) with the organozinc species (**2**). While the experimental geometry of ethene is well reproduced by both DFT functionals, no clear-cut experimental information about the structure of **2** is available. Irrespective of the functional applied, our calculations identify the cyclopropanating agent as a C_s-symmetric diiodomethane with the zinc inserted into one of the carbon iodine bonds. The C–Zn–I moiety adopts a linear arrangement with Zn–I and Zn–C bond distances in the expected range. In their recent X-ray crystallographic investigation of the related bis(iodomethyl)zinc intermediate, complexed with a glycol ether, Denmark *et al.*[7] report Zn–C and C–I bond lengths between 1.92 and 2.02 Å and 2.13 and 2.21 Å, respectively. The I–C–Zn angle has been determined as 107.4°–116.1°, again in good agreement with the corresponding calculated angles of 107.4° (BP) and 108.9° (BLYP) in the monomeric species **2**. Assuming that the Simmons–Smith reaction is indeed concerted, the interaction between **1** and **2** should lead directly to the products, *i.e.* ZnI_2 (**3**) and cyclopropane (**4**) *via* a single transition state. This transition state should be characterized by a—not necessarily symmetric—interaction between the carbon atoms of the ethene substructure and the carbon atom of **2** with a concomitant breaking of the C–I and C–Zn bonds and the formation of the second Zn–I bond in the carbenoid. Thus, in the transition state the 'leaving group' ZnI_2 will be preformed at the same time as the cyclopropane moiety is being generated. On the other hand, should this reaction occur stepwise, at least one intermediate should exist along the reaction coordinate. Our search for a concerted transition structure led to the localization of **TS1** (C_s point group symmetry), which is characterized by one negative eigenvalue in the force constant matrix and a corresponding imaginary frequency of 278i and 269i cm^{-1} with the BP and BLYP functionals, respectively. Fig. 2 displays the transition vector, *i.e.* the normal mode associated with the imaginary frequency which describes the reaction coordinate at the saddle point. It clearly corresponds to a motion of the ethene carbons towards the carbenoid carbon atom. The approach is not symmetric, the C^1–C^2 distance is some 0.26–0.27 Å shorter than the C^1–C^3 distance. A significant pyramidalization of more than 8° occurs at C^2, indicating the onset of the $sp^2 \longrightarrow sp^3$ rehybridization required for the cyclopropane formation. An important structural aspect of **TS1** is the significant decrease of the I^1–C^1–Zn angle from some 108° in **2** to only 70.4° (BP) or 67.9° (BLYP). This goes hand in hand with a lengthening of the carbon–iodine bond by a substantial amount of 0.486 Å or even 0.587 Å using the BP and BLYP functionals, respectively and a concomitant shortening of the I^1–Zn distance from 3.392 (BP) and 3.449 Å (BLYP) in **2** to 2.772 (BP) and 2.781 Å (BLYP) in **TS1**. Obviously, all these structural features can be attributed to the formation of a ZnI_2 moiety in the saddle point. It should be noted that the structure of this transition state bears strong

Table 2 Calculated total and relative energies

	BP		BLYP		ADF/BP[a]
	E_{tot}/hartree	E_{rel}/kJ mol^{-1}	E_{tot}/hartree	E_{rel}/kJ mol^{-1}	E_{rel}/kJ mol^{-1}
1	−78.579 38	0.0	−78.537 12	0.0	0.0
2	−128.177 41		−127.947 33		
TS1	−206.738 31	48.5	−206.463 16	55.9	61.1
5	−206.827 90	−187.7	−206.543 80	−155.9	−142.7
3	−88.929 47	−158.3	−88.723 76	−140.0	−142.3
4	−117.887 59		−117.814 00		
TS2	−206.746 64	26.7	—[b]	—	59.8
6	−206.805 54	−128.0	−206.522 25	−99.3	−108.4

[a] ADF does not provide total, but only energies relative to user-defined fragments. [b] Not computed due to technical problems, see text.

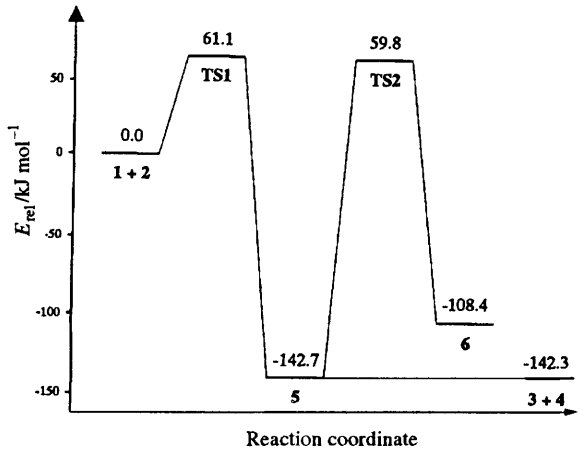

Fig. 3 Potential energy surface computed at the ADF/BP level for the Simmons–Smith reaction. Energies given in kJ mol^{-1}.

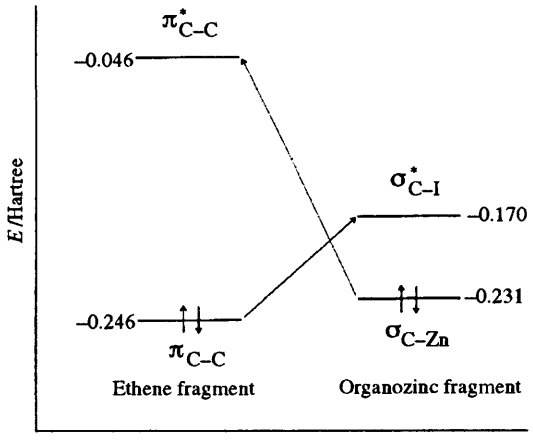

Fig. 4 Frontier molecular orbital interactions in **TS1**

similarity to intermediate points along the reaction coordinate of the addition of singlet methylene to ethene to form cyclopropane. This reaction has been extensively studied by Reuter *et al.*[22] employing sophisticated multireference configuration interaction calculations. The addition is continuously exothermic and thus without an activation barrier. However, due to unfavourable orbital overlap the CH_2 attack does not follow a C_{2v} path perpendicular to the double bond. Rather, one of the two ethene carbon atoms is attacked preferentially and the methylene hydrogens are bent towards the other carbon atom. It is only in the last part of the reaction coordinate that the CH_2 unit assumes its final orientation.[22]

While **TS1** has all the features expected for the saddle point of a concerted reaction, it nonetheless cannot be ruled out that it connects the educts with an intermediate which only in a subsequent step leads to the products. For example, **TS1** could be *en route* to an intermediate where only the C^1–C^3 bond has been formed and C^1 is connected to a ZnI_2 unit. In fact, such a structure has been localized as a stationary point (**TS2**), but the analysis of the force constant matrix revealed that it represents a saddle point rather than a minimum (see below). In order to unambiguously establish the role of **TS1** in the reaction, we computed the intrinsic reaction coordinate (IRC)[23] which allows the identification of the minimum structures which are connected through a particular saddle point. While following the IRC in one direction leads back to the educts, the endpoint of the second direction was the C_{2v} symmetric species **5**. This structure represents an electrostatically bound complex between cyclopropane and ZnI_2 which is of course the direct precursor to the separated products. Thus, as anticipated, **TS1** is indeed the saddle point for the concerted pathway of the Simmons–Smith reaction. The activation barrier, *i.e.* the relative energy of **TS1** with respect to the educts, amounts to 48.5 (BP) or 55.9 kJ mol^{-1} (BLYP). If, instead of the RECP, the ADF based quasi-relativistic approach with the BP functional is employed to compute this relative energy, the activation barrier increases only slightly to 61.1 kJ mol^{-1}. The electrostatic complex **5** is 187.7 (BP), 155.9 (BLYP) and 142.7 (ADF/BP) kJ mol^{-1} below the educts, while the separated products are theoretically predicted to be 158.3 (BP), 140.0 (BLYP) and 142.3 (ADF/BP) kJ mol^{-1} more stable than the sum of **1** and **2**. However, the surprisingly large stability of **5** with respect to the separated products in the RECP calculations (BP and BLYP) is an artifact due to the basis set superposition error (BSSE)[24] and reflects the rather small valence basis set used. After correction for the BSSE through the standard counterpoise procedure[25] the complex **5** is only marginally more stable than the sum of the isolated products **3** and **4**. This problem does not occur at the ADF/BP level of approximation, since a significantly larger one particle basis set is employed. The presence of **5** is most likely a consequence of the absence of a solvent and therefore restricted to the gas phase. If the interaction of a solvent is taken into account, **5** will certainly disappear.[26] While the above calculations establish a concerted pathway with an activation barrier of around 59 kJ mol^{-1}, the problem still remains whether other, more complicated but perhaps energetically more favourable mechanisms exist. To settle this question we carefully searched the relevant part of the potential energy surface for possible intermediate structures and/or saddle points. The only reasonable minimum structure located was **6**, which represents the propane analogue of the original Simmons–Smith reagent. IRC calculations indicated that **6** is reached *via* **TS2** from the complex **5**. However, to generate cyclopropane and ZnI_2 from **6**, the C^1–C^3 and Zn–I^2 bond has to be formed with concomitant breaking of the Zn–C^1 bond and no simple path to the products could be found. Hence, **6** must be regarded as a dead-end in the context of the Simmons–Smith reaction. We note in passing that while in **2** the I–Zn–C angle is linear, in **6** this angle is only around 160°. From an energetic point of view, **TS2** is similar to **TS1**, being 26.7 (BP) and 59.8 (ADF/BP) kJ mol^{-1} above the educts (for technical reasons, no BLYP calculations could be performed on this

species), while **6** is 128.0 (BP), 99.3 (BLYP) and 108.4 (ADF/BP) kJ mol^{-1} below the energy of **1** + **2** and thus some 29–42 kJ mol^{-1} above the products. Using the ADF/BP data as probably the most reliable ones, the potential energy surface as shown in Fig. 3 can be constructed for the mechanism of the solvent-free Simmons–Smith reaction.

The mechanistic scenario with **TS1** as the key species presented above also explains two other experimentally known features of the Simmons–Smith reaction. In contrast to the free carbene addition the yields do depend on the steric situation around the double bond. For example, only the sterically less crowded exocyclic, but not the endocyclic double bond, is attacked in the reaction with D-limonene. This selectivity is obviously a consequence of the sterically demanding structure of **TS1**. The second observation is that the cyclopropanating species reacts more readily with electron-rich double bonds and thus acts as an electrophile in the Simmons–Smith reaction. This can easily be rationalized by employing simple frontier molecular orbital[27] (FMO) arguments. If we divide **TS1** into two fragments corresponding to **1** and **2** (but in the geometry these fragments adopt the saddle point), two modes of FMO interactions are conceivable. Either, the occupied π-orbital of ethene interacts with the empty σ*-C–I orbital on the cyclopropanating reagent or the interaction takes place between the virtual π*-orbital of ethene and the occupied σ-C–Zn orbital of ICH_2ZnI. While the former interaction is indicative of an electrophilic attack of **2**, in the latter **2** acts as the nucleophile. As depicted in Fig. 4, the interaction between the two fragments corresponding to an electrophilic attack of **2** is indeed by far more favourable than the nucleophilic alternative, supporting the experimentally deduced mode of interaction.

Conclusions

The following conclusions can be drawn from our quantum chemical study employing density functional theory and including scalar relativistic effects. (i) A concerted gas phase mechanism for the Simmons–Smith cyclopropanation reaction is predicted. (ii) A transition state with similar geometric features as computed for intermediate structures along the reaction coordinate for the barrier free addition of singlet carbene to ethene has been identified for this concerted mechanism. (iii) The activation barrier for this pathway amounts to 48–61 kJ mol^{-1}, depending of the functional employed. (iv) The overall exothermicity is between 140 and 158 kJ mol^{-1}. (v) In agreement with experimental information, the mode of attack of the cyclopropanating species is electrophilic in nature.

Acknowledgements

This work was financially supported by the Fonds der Chemischen Industrie. Computer time and excellent service was generously provided by the Zentraleinrichtung Rechenzentrum der Technischen Universität (R. Gülker) and by Professor A. Fortenbacher, Fachhochschule für Technik und Wirtschaft Berlin. Finally, we thank R. H. Hertwig and M. C. Holthausen for many helpful discussions.

References

1 (*a*) H. E. Simmons and R. D. Smith, *J. Am. Chem. Soc.*, 1958, **80**, 5323; (*b*) 1959, **81**, 4256; (*c*) E. P. Blanchard and H. E. Simmons, *J. Am. Chem. Soc.*, 1964, **86**, 1337; (*d*) H. E. Simmons, E. P. Blanchard and R. D. Smith, *J. Am. Chem. Soc.*, 1964, **86**, 1347.
2 G. Emschwiller, *C. R. Seances Acad. Sci.*, 1929, **188**, 1555.
3 G. Wittig and K. Schwarzenbach, *Angew. Chem.*, 1959, **71**, 652; *Liebigs Ann. Chem.*, 1962, **650**, 1; G. Wittig and F. Wingler, *Liebigs Ann. Chem.*, 1962, **656**, 18; *Chem. Ber.*, 1964, **97**, 2146; G. Wittig and M. Jautelat, *Liebigs Ann. Chem.*, 1967, **702**, 24.
4 J. Furukawa, N. Kawabata and J. Nishimura, *Tetrahedron Lett.*, 1966, 3353; *Tetrahedron*, 1968, **24**, 53; J. Nishimura, J. Furukawa, N. Kawabata and M. Katayama, *Tetrahedron*, 1971, **27**, 1799.
5 H. E. Simmons, T. L. Cairns and S. A. Vladuchick, *Org. React. (N. Y.)*, 1973, **20**, 1.
6 See, *e.g.* J. March, *Advanced Organic Chemistry*, Wiley-Interscience, Chichester, 1992, p. 870.
7 S. E Denmark, J. P. Edwards and S. R. Wilson, *J. Am. Chem. Soc.*, 1991, **113**, 723; 1992, **114**, 2592.
8 See, *e.g.* R. G. Parr and W. Yang, *Density Functional Theory of Atoms and Molecules*, Oxford University Press, New York, 1989.
9 J. C. Slater, *Phys. Rev.*, 1951, **81**, 285.
10 S. J. Vosko, L. Wilk and M. Nusair, *Can. J. Phys.*, 1980, **58**, 1200.
11 A. D. Becke, *J. Chem. Phys.*, 1986, **84**, 4524.
12 J. P. Perdew, *Phys. Rev. B: Condens. Matter*, 1986, **33**, 8822.
13 C. Lee, W. Yang and R. G. Parr, *Phys. Rev. B: Condens. Matter*, 1988, **37**, 785.
14 Zn: P. J. Hay and W. R. Wadt, *J. Chem. Phys.*, 1985, **82**, 270; I: W. R. Wadt and P. J. Hay, *J. Chem. Phys.*, 1985, **82**, 284.
15 A. Höllwarth, M. Böhme, S. Dapprich, A. W. Ehlers, A. Gobbi, V. Jonas, K. F. Köhler, R. Stegmann, A. Veldkamp and G. Frenking, *Chem. Phys. Lett.*, 1993, **208**, 237.
16 P. C. Hariharan and J. A. Pople, *Theor. Chim. Acta*, 1973, **28**, 213.
17 G. Frenking, I. Antes, M. Böhme, S. Dapprich, A. W. Ehlers, V. Jonas, A. Neuhaus, M. Otto, R. Stegmann, A. Veldkamp and S. F. Vyboishchikov, in *Reviews* in *Computational Chemistry*, eds. K. B. Lipkowitz and D. B. Boyd, VCH, Weinheim, vol. VIII, 1996.
18 GAUSSIAN92/DFT Rev. F.2: M. J. Frisch, G. W. Trucks, H. B. Schlegel, P. M. W. Gill, B. G. Johnson, M. W. Wong, J. B. Foresman, M. A. Robb, M. Head-Gordon, E. S. Replogle, R. Gomperts, J. L. Andres, K. Raghavachari, J. S. Binkley, C. Gonzales, R. L. Martin, D. J. Fox, D. J. Defrees, J. Baker, J. J. P. Stewart and J. A. Pople, GAUSSIAN Inc., Pittsburgh, 1992.
19 T. Ziegler, V. Tschinke, E. J. Baerends, J. G. Snijders and W. Ravenek, *J. Phys. Chem.*, 1989, **93**, 3050.
20 ADF version 1.1.3, G. TeVelde and E. J. Baerends, *J. Comput. Phys.*, 1992, **99**, 84 and literature cited therein.
21 For a similar situation see the recent discussion of $PdCH_2I^+$: J. Schwarz, C. Heinemann, D. Schröder, H. Schwarz and J. Hrušák, *Helv. Chim. Acta*, 1996, **79**, 1.
22 W. Reuter, B. Engels and S. D. Peyerimhoff, *J. Phys. Chem.*, 1992, **96**, 6221.
23 K. Fukui, *J. Phys. Chem.*, 1970, **74**, 4161; *Acc. Chem. Res.*, 1981, **14**, 363.
24 B. Liu and A. D. McLean, *J. Chem. Phys.*, 1973, **59**, 4557; F. B. van Duijneveldt, J. G. C. M. van Duijnefeldt-van de Rijdt and J. H. van Lenthe, *Chem. Rev.*, 1994, **94**, 1873.
25 S. F. Boys and F. Bernardi, *Mol. Phys.*, 1970, **19**, 553.
26 Compare the similar situation when comparing the gas phase mechanism of the S_N2 reaction with the mechanism in a solvent: S. S. Shaik, H. B. Schlegel and S. Wolfe, *Theoretical Aspects of Physical Organic Chemistry. The S_N2 Mechanism*, Wiley, Chichester, 1992.
27 See, *e.g.* K. Fukui, *Theory of Orientation and Stereoselection*, Springer Verlag, Berlin, 1975.

Paper 5/06644A
Received 9*th October* 1995
Accepted 12*th January* 1996